AFRL-RZ-WP-TP-2008-2035

SPRAY STRUCTURE IN NEAR-INJECTOR REGION OF AERATED JET IN SUBSONIC CROSSFLOW (POSTPRINT)

J. Lee, K.A. Sallam, K.-C. Lin, and Campbell D. Carter

Propulsion Sciences Branch
Aerospace Propulsion Division

JANUARY 2008

AIR FORCE RESEARCH LABORATORY
PROPULSION DIRECTORATE
WRIGHT-PATTERSON AIR FORCE BASE, OH 45433-7251
AIR FORCE MATERIEL COMMAND
UNITED STATES AIR FORCE

REPORT DOCUMENTATION PAGE

Form Approved
OMB No. 0704-0188

1. REPORT DATE *(DD-MM-YY)*	2. REPORT TYPE	3. DATES COVERED *(From - To)*
January 2008	Conference Paper Postprint	30 April 2004 – 01 December 2006

4. TITLE AND SUBTITLE
SPRAY STRUCTURE IN NEAR-INJECTOR REGION OF AERATED JET IN SUBSONIC CROSSFLOW (POSTPRINT)

5a. CONTRACT NUMBER
In-house

5b. GRANT NUMBER

5c. PROGRAM ELEMENT NUMBER
61102F

6. AUTHOR(S)
J. Lee and K.A. Sallam (Oklahoma State University)
K.-C. Lin (Taitech, Inc.)
Campbell D. Carter (AFRL/RZAS)

5d. PROJECT NUMBER
2308

5e. TASK NUMBER
AI

5f. WORK UNIT NUMBER
2308AI00

7. PERFORMING ORGANIZATION NAME(S) AND ADDRESS(ES)

Oklahoma State University
Stillwater, OK, 74078

Taitech, Inc.
Beavercreek, OH 45433

Propulsion Sciences Branch (AFRL/RZAS)
Aerospace Propulsion Division
Air Force Research Laboratory, Propulsion Directorate
Wright-Patterson Air Force Base, OH 45433-7251
Air Force Materiel Command, United States Air Force

8. PERFORMING ORGANIZATION REPORT NUMBER
AFRL-RZ-WP-TP-2008-2035

9. SPONSORING/MONITORING AGENCY NAME(S) AND ADDRESS(ES)

Air Force Research Laboratory
Propulsion Directorate
Wright-Patterson Air Force Base, OH 45433-7251
Air Force Materiel Command
United States Air Force

10. SPONSORING/MONITORING AGENCY ACRONYM(S)
AFRL/RZAS

11. SPONSORING/MONITORING AGENCY REPORT NUMBER(S)
AFRL-RZ-WP-TP-2008-2035

12. DISTRIBUTION/AVAILABILITY STATEMENT
Approved for public release; distribution unlimited.

13. SUPPLEMENTARY NOTES
Conference paper published in the Proceedings of the 46th AIAA Aerospace Sciences Meeting and Exhibit.

 Report contains color.

PAO Case Number: WPAFB 07-0706, 17 Dec. 2007.

14. ABSTRACT
An experimental study of the breakup of aerated liquid jet in subsonic crossflow was carried out. The test conditions were as follows: jet exit diameter of 1 mm, GLR (gas to liquid ratio) of 8%, and jet-to-free stream momentum flux ratio of 0.74. Digital double-pulsed holograms were recorded at x/do = 0 to 25 in the cross stream direction, y/do = 0 to 27 in the stream wise (injection direction), and z/do = (-13) to 13 in the span-wise direction. Digital double-pulsed holographic microscopy (DHM) was utilized using double exposure 2048x2048 pixels CCD sensor. The field of view of all holograms was 9 mm x 9 mm, and the spatial resolution was 5 μm. To overcome this small field of view, three-dimensional spray maps were constructed by patching several high resolution holograms. Measurements include droplets locations, drop sizes and sphericity, and three-dimensional velocities. The distributions of the drop sizes could be fully described by the SMD alone and followed Simmons' universal root-normal distribution.

15. SUBJECT TERMS

16. SECURITY CLASSIFICATION OF:			17. LIMITATION OF ABSTRACT:	18. NUMBER OF PAGES	19a. NAME OF RESPONSIBLE PERSON (Monitor)
a. REPORT	b. ABSTRACT	c. THIS PAGE			Campbell D. Carter
Unclassified	Unclassified	Unclassified	SAR	26	19b. TELEPHONE NUMBER *(Include Area Code)* N/A

Standard Form 298 (Rev. 8-98)
Prescribed by ANSI Std. Z39-18

46th AIAA Aerospace Sciences Meeting and Exhibit
7 - 10 January 2008, Reno, Nevada

AIAA-2008-1043

Spray Structure in Near-Injector Region of Aerated Jet in Subsonic Crossflow

J. Lee[1] and K.A. Sallam[2]
Oklahoma State University, Stillwater, Oklahoma, 74078

K.-C. Lin[3]
Taitech Inc., Beavercreek, Ohio 45433

and

C.D. Carter[4]
Air Force Research Laboratory, Wright-Patterson AFB, Ohio 45433

An experimental study of the breakup of aerated liquid jet in subsonic crossflow was carried out. The test conditions were as follows: jet exit diameter of 1 mm, GLR (gas to liquid ratio) of 8%, and jet-to-free stream momentum flux ratio of 0.74. Digital double-pulsed holograms were recorded at x/d_o = 0 to 25 in the cross stream direction, y/d_o = 0 to 27 in the stream wise (injection direction), and z/d_o = (-13) to 13 in the span-wise direction. Digital double-pulsed holographic microscopy (DHM) was utilized using double exposure 2048×2048 pixels CCD sensor. The field of view of all holograms was 9 mm × 9 mm, and the spatial resolution was 5 µm. To overcome this small field of view three-dimensional spray maps was constructed by patching several high resolution holograms. Measurements include droplets locations, drop sizes and sphericity, and three-dimensional velocities. The distributions of the drop sizes could be fully described by the SMD alone and followed Simmons' universal root-normal distribution. The distributions of the stream wise and cross stream velocities were uniform in the near-injector region and could be characterized by the mass-average velocity except for very small and very large droplets.

Nomenclature

d	= drop diameter
d_0	= injector orifice diameter
q_0	= jet/freestream momentum flux ratio, $\rho_L^2 v_j^2 / \rho_\infty^2 u_\infty^2$
GLR	= aerating gas-to-liquid mass flow rate ratio
SMD	= Sauter mean diameter, $\Sigma d_i^3 / \Sigma d_i^2$
MMD	= mass median diameter
u	= velocity component in the crossflow (horizontal) direction
U_∞	= freestream velocity

[1] Graduate student, Mechanical and Aerospace Engineering.
[2] Assistant Professor, Mechanical and Aerospace Engineering. Senior Member AIAA. Corresponding Author: Tel: 405-762-0749, Email: khaled.sallam@okstate.edu (K.A. Sallam).
[3] Senior Research Scientist. Associate Fellow AIAA.
[4] Senior Aerospace Engineer. Member AIAA.

v = velocity component in the jet streamwise (vertical) direction
v_j = jet exit velocity
w = velocity component in the jet spanwise (normal to the page) direction
x = cross-stream (horizontal) distance from the injector exit
y = streamwise (vertical) distance from the injector exit
z = spanwise (normal to the page) distance from the injector exit
ρ = density
$\Delta\xi$ = hologram resolution
λ = wave length
N = the number of pixels
Δx = the pixel size

Subscripts:
G = aerating gas property
j = jet exit property
L = liquid property
∞ = freestream property

Superscripts:
$\sim$ = mass averaged properties

I. Introduction

A good understanding of the phenomena of liquid jet breakup is essential for successful design of gas turbine fuel injectors, ramjet and scramjet engines, diesel fuel injectors, medical sprays, and inkjet printers, among others. The major objective of most injectors is to atomize a liquid jet into a fine spray. Pressure atomizers, such as plain orifice nozzle injector, accomplish this objective by using very small orifice diameter and/or very high injection pressure. In many applications this solution is not feasible, because small orifice diameters tend to get clogged easily and high injection pressure is not always available. Aerated liquid injector (also known as effervescent atomizer), on the other hand, can easily provide dense sprays of fine droplets with low injection pressures and large orifice diameter by introducing gas bubbles into liquid stream inside an injector. Aerated injection is similar to the flash atomization because it produces gas bubbles inside the injector for promoting atomization. However, unlike flash atomizers, aerated injection can easily control the amount of bubbles and their sizes without the complications of dissolving gas or heating the liquid to its boiling point. The aerated liquid injector allows large exit orifice diameter because atomization quality depends on liquid sheet thickness rather than the orifice diameter. Moreover, the aerated atomization generates fine spray at low injection pressures and low gas flow rates for a wide range of operating viscosities.

The dense spray region near the injector is optically-opaque for Phase Doppler Interferometry, e.g. Phase Doppler Particle Analyzers (PDPA). Moreover, two-dimensional methods, e.g. shadowgraphy, have limited depth-of-field that renders them impractical for measuring droplet sizes and velocities of three-dimensional spray structure. Miller et al.[1] have successfully used digital holography to probe the droplets sizes of aerated liquid jet in crossflow at downstream distances between $x/d_0 = 25$ and $x/d_0 = 50$ using single laser beam. They used two methods which are digital inline holography (DIH) and digital holographic microscopy (DHM) (also known as digital microscopy holography), and demonstrated that two methods are suitable for measuring the properties of the dense spray region and insensitive to the non-spherical droplets. They concluded that DHM is the best method for providing valuable information about the small droplets encountered in the spray because of its ability to resolve very small details. In spite of their efforts, however, there is still lack of data on droplets velocities in the near field. There is also lack of data on droplets sizes and droplets' velocities very near the aerated injector ($x/d_0 < 25$).

Kim and Lee [2] studied the two phase internal flow pattern inside the aerated injector for different GLRs by using a transparent aerated injector and a pulsed shadowgrpahy. The flow patterns inside the aerated injector could be classified into three regimes as follows: bubbly flow regime, intermittent flow regime, and annular flow regime. When the GLR is small, the flow pattern inside the injector becomes bubbly because small bubbles are distributed throughout the liquid. However, at a large value of GLR, a liquid layer is formed along the wall of the injector exit passage and the internal flow pattern becomes annular. At the intermediate GLR, the internal flow pattern randomly wanders between the bubbly flow and annular flow regimes.

Lefebvre et al.[3] investigated the influences of nozzle geometric design on atomization performance. They concluded that exit orifice diameter has little effect on the mean droplet sizes. Buckner and Sojka[4] investigated

effervescent atomization of high viscosity fluids in the annular flow regime. They concluded that mean droplet diameter is sensitive to GLR (Gas Liquid Ratio) but nearly independent of liquid viscosity, fluid supply pressure, and mixture mass flow rate. Lund et al.[5] reported the influence of surface tension on effervescent atomization. They found that drop size decreases with an increase in surface tension.

Santangelo and Sojka[6] investigated the near nozzle spray structure of an effervescent atomizer using focused image holography. They divided the spray structure into three flow regimes based on the GLRs. In bubbly flow regime, GLR < 2%, the breakup process is governed by individual bubble expansion. A cylinder of liquid (a trunk) breaks up into ligaments and droplets due to individual bubble expansion. In transition flow regime the trunk became distorted and was replaced by a ring of limbs, which formed a tree. In the annular flow regime, the trunk is greatly reduced in length, and a small number of large limbs break up into a higher number of thinner limbs and branches. Sutherland et al.[7] reported entrainment of ambient air into the spray produced by ligament controlled effervescent atomizer. The advantage of this atomizer is to get mean drop sizes below 70 μm, to reduce atomizing air consumption by less than 0.009, and to remove the effect of surface tension and viscosity on the atomizer performance. They found that entrainment number which is function of steady entrainment rate and momentum rate is insensitive to liquid physical properties but increases with GLR. Wade et al.[8] reported that the spray characteristics of an effervescent atomizer operating in the MPa injection pressure ranges. The Sauter mean diameter (SMD) decreases with the increase in injection pressure and the increase of exit orifice diameter. Spray cone angle was not influenced by the exit orifice diameter but increased with the increase of GLR and the injection pressure.

Lin et al.[9,10] studied the spray structure of the aerated liquid jet in crossflow using PDPA and pulsed shadowgraphy. They reported that as the GLR increased, the droplet distribution in the spray plume changed from multi-dispersed to mono-dispersed. They also suggested the following correlation for the penetration height of the aerated liquid jet injected in crossflow. Sallam et al.[11] investigated primary breakup of round aerated liquid jets in supersonic crossflow using single- and double-pulsed shadowgraphy and holography. For GLR greater than 2%, the aerated liquid jet was in the annular flow regime, and spray cone angle and surface breakup properties along upstream and downstream of the liquid sheet were similar indicating weak aerodynamic effect. They developed a correlation for the aerated liquid sheet thickness. Miller et al.[1] used two injector exit diameters of 1mm and 5mm, GLR of 4% and 8%, jet-to-freestream momentum ratios of 0.74 and 4 to investigate the spray structure at two locations of 25 and 50 jet diameters. The increase in GLR from 4% to 8% reduced the SMD probably due to the squeezing effect of the liquid sheet. The variation of the exit diameters influenced the number of droplets produced as was shown by the liquid volume fraction plots. The jet-to-freestream momentum flux ratio had an effect on controlling the spray plume penetration. At the same GLR, the SMD was reduced between two different downstream locations of $x/d_0 = 25$ and $x/d_0 = 50$. They suggested that this effect was due to the secondary breakup. However, they did not perform any velocity measurements and therefore could not measure the Weber number of the droplets in the near field. A velocimetry technique is needed to measure the Weber number of these drops to determine whether secondary breakup mechanism is indeed active in this region.

II. Experiment Method

A. Apparatus

The aerated liquid jet breakup experiments were performed in a subsonic wind tunnel with a test section of 0.3 m × 0.3 m × 0.6 m. This test section had float glass side walls and floor, and acrylic ceiling to provide optical access. The range of air velocities was from 3 m/s to 60 m/s at normal temperature and pressure. The wind tunnel's contraction ratio is 16:1, and the velocity inside the test section has a variation within ± 1 % of the mean free-stream velocity. Air velocities in the wind tunnel could be measured within ± 2 %. The test liquid was supplied from a cylindrical chamber (constructed of type 304 stainless steel) having a diameter of 100 mm and a height of 300 mm, and the aerating gas for mixing with the liquid was provided from a stainless steel static pressure tank with a volume of 0.18 m^3 and an air pressure limit up to 5000 kPa. An aerated injector has been installed on the acrylic ceiling of the test section to provide optical access. The exit diameters (d_0) of the aerated liquid injector used for this research were 1.0 mm. Aerating gas supplied from the storage tank comes in to meet with the liquid inside the nozzle by traveling through the inner tube and passing through 100 μm holes located near the end of the injector as shown in Figure 1. The jet, at sufficient GLR (greater than 2%), forms an annular-type spray of two-phase flow composed of a gas core surrounded by a thin liquid sheet. Air pressures up to 1.1 Mpa was used in the aerating gas, and water, also pressurized to 1.1 Mpa, was used as the liquid.

The schematic diagram of experimental apparatus including optical setup is shown in Figure 2. The flow rate of liquid and aerating gas for effective GLR was controlled by a rotameter type flow meter. The reading error of air

flow rate was within ± 3 cc/s, and that of water flow meter was within ± 0.02 cc/s. Therefore, the maximum uncertainty in the gas flow rate measurement is 28% and the maximum uncertainty in the liquid flow rate measurement is 6%. An aluminum black bread board was installed under the wind tunnel test section for easy routing of the double pulsed lasers from an optical table to the wind tunnel test section. Moreover, this breadboard has a rail that can be moved horizontally. This was used to transverse the CCD camera and the objective lens and the spatial filter assembly with 1 mm accuracy. The schematic of double pulsed digital holographic microscopy is shown in Figure 3. The holograms were captured on a Cooke Corporation cooled interline transfer CCD camera (Model : PCO 2000) having 2048 × 2048 pixels. Two laser pulses were synchronized with the double exposure time of CCD by a pulse generator. Two frequency doubled Nd:YAG lasers (Spectra Physics Model LAB-150, 532 nm wavelength, 7 ns pulse duration, and up to 300 mJ optical energy per pulse) that could be fired with a pulse separation as small as 100 ns were used as the light source. The two laser beams were aligned with a polarized beam splitter cube, and their intensities were controlled by two half wave plates as shown in Figure 3. A photo detector and an oscilloscope (Lecroy model 9314L, 300Hz bandwidth, 1Mpt memory depth, 100Ms/s sample rate) were used to measure the separation time between the two pulses. An objective lens (M 5x) and a 15 μm pinhole were used to expand the laser beam for digital holographic microscopy. The distance from the light source to the CCD was recorded within 1 mm accuracy during the test since it is needed for the digital reconstruction process. The resolution of the digital hologram depends on the distance from the object to the CCD, the wavelength of the light, and the pixel size of the CCD. The resolution of the hologram is determined by Schnars and Jueptner[12] as follows:

$$\Delta\xi = \lambda d / N\Delta x \tag{1}$$

where $\Delta\xi$ is the resolution, λ is the wave length, d is the recording distance, i.e. the distance from the object to the CCD, N is the number of pixels, and Δx is the pixels size. The distance between the objective lens and aerated jet was minimized for good resolution, and the distance between the aerated jet and CCD sensor was minimized for good field of view. The total distance between objective lens and CCD sensor was 550mm. All double-pulsed holograms were recorded at the range of $x/d_0 = 0 \sim 31.5$ and $y/d_0 = 0 \sim 63$.

B. Instrumentation and Measuring Technique

When the digital hologram is stored on the CCD sensor, it can be easily reconstructed by a numerical algorithm (Schnars and Jueptner, 2005). After the reconstruction process, three-dimensional volume information is expressed by many reconstruction holograms focused on each two-dimensional plane. Because of the expanding laser beam used for DHM, the spatial calibration is continuously changing for each one of these two-dimensional planes. To conduct the spatial calibration, one needs at least three pins placed at three different distances from the CCD sensor. In the present study, four pins with the same diameter (d_{pin} = 0.5mm) as shown in Figure 4 were used to spatially calibrate the reconstructed holograms. The spacing among four pins was respectively 5 mm in the span wise direction, i.e., laser beam direction. The hologram for spatial calibration was obtained with a distance of 550 mm between objective lens and CCD, and the Q-switch laser energy used was 52.8 mJ/pulse. Figure 5a shows the original hologram of four pins and reconstruction two dimensional image at the depth of 76 mm. When a pin on the original hologram is reconstructed in a two-dimensional plane, the others are out of focus. The second pin in Fig. 5b is very focused, but the other pins are out of focus because this hologram was reconstructed at the depth of 76 mm. Four pins have been consecutively reconstructed with 3 mm distance interval of ranging from 70 mm to 79 mm as shown in Fig. 6. In other words, actual distance (the spacing of four pins) is 5 mm, but each pin was reconstructed with the distance interval of 3 mm. The span-wise actual distance was determined by this ratio. Because of expanding laser beam diameter, the reconstructed image of each of the identical four pins had different diameter. Fig. 6 shows the spatial calibration relationship used in the present study. The linear correlation of Fig. 6 is as follows:

$$Y = -0.0213X + 5.5914 \tag{2}$$

where Y is the ratio of pin diameters (μm/pixels) and X is the reconstruction distance (mm). The stream-wise actual distance and cross-sectional actual distance can be calibrated with this equation by counting pixel number for all reconstruction holograms. Thus, this equation becomes very useful for getting the actual distance in each reconstruction two-dimensional plane.

The smallest droplets with diameters of 12 μm were measured with uncertainties of 73 %. For the smallest SMD of 40 μm was measured with uncertainty of 22%. Uncertainty in locating droplet position in the spanwise direction depends on how well the droplets plane of focus can be found. Since reconstructions were made with 0.17 mm

increments in the spanwise direciton, the location of the centroid of the droplet can be known within ± 0.17 mm. Measurements in the cross-sectional and streawmwise direction were determined by the placement of the camera when the holograms were recorded. The location of the camera could be determined within ± 1 mm.

C. Test Condition

The aerated injector with the exit diameter of 1 mm was tested at the GLR of 8%. To maintain a GLR of 8%, a water flow rate of 87mL/min and an air flow rate of 6181mL/min were used. The aerating gas used was pressurized to 1.1 MPa and the liquid used was tap water also pressurized to 1.1 MPa. The properties of the water were as follows: density = 999 kg/m^3, surface tension = 0.00734 N/m, kinematic viscosity = 1.12 x 10^{-6} m^2/s. To hold the jet-to-freestream momentum flux ratio (q_0) at 0.74, the wind tunnel was set to a speed of u_∞ = 61 m/s.

Holograms were digitally recorded at the range of $x/d_0 = 0 \sim 31.5$ and $y/d_0 = 0 \sim 63$ to probe the near injector region of the aerated liquid jet. The field of view of the holograms with high resolution was 9 mm × 9 mm. To overcome this limited field of view, the dense spray region of $x/d_0 = 0 \sim 31.5$ and $y/d_0 = 0 \sim 63$ was divided into several investigation windows. At each of the investigation windows holograms were recorded starting at the top of the test section and then moving the CCD sensor and the objective lens down in 9 mm increments which is the height of the CCD sensor. The CCD sensor continued to be lowered until no more droplets appeared.

After the holograms were digitally recorded, they were then reconstructed at span wise distances at increments of ± 0.17 mm throughout the spray volume. The reconstruction range was determined such that it could cover all the droplets in the spray at that particular location. The maximum range of reconstruction depth of spanwise direction was ± 13mm. In each of the reconstruction holograms the focused droplets were used to measure droplets diameters, locations, and three-dimensional velocities. The SMD was then calculated by averaging the droplets diameters over five span wise incremental distances which are the equivalent of 0.83 mm.

III. Results and Discussion

Double-pulsed digital holographic microscopy (DHM) was used for probing the dense-spray near-injector region of aerated liquid jet in crossflow. To overcome the limited field of view, the dense-spray region (x/d_0=0~22.5 and y/d_0=0~27) has been divided into nine investigation windows. Droplets' diameters, locations, and three-dimensional velocities were measured in these nine investigation windows. The test conditions were GLR of 8%, jet-to-freestream momentum flux ratio (q_0) of 0.74, and injector exit diameter (d_0) of 1 mm. For the flow visualization of the region of x/d_0=0~22.5 and y/d_0=0~27 the spray structure map has been constructed by patching six high resolution holograms reconstructed at the same spanwise (distance from the camera) depth. Droplets' sizes and three-dimensional velocities could be expressed together on the same plot. The majority of the droplets in the near-injector region were elliptical, and they were characterized using equivalent diameters. Mass averaged velocities were successful to describe the structure of aerated liquid jets.

A. Flow Visualization

A pulsed shadowgraph of aerated liquid jet in subsonic crossflow is shown in Fig. 8. This shadowgraph was obtained at the following test condition: nozzle orifice diameter of 1 mm, gas to liquid ratio (GLR) of 8%, and jet-to-freestream momentum flux ratio (q_0) of 0.74. Despite the high resolution of the shadowgraph achieved by using large format (127mm×127mm) film, this shadowgraph has limited depth of field, typical of large magnification shadowgraphy. The shadowgraph projects three-dimensional spray structure of aerated liquid jet into two-dimensional spray with many drops out of focus due to the limited depth of field. To overcome the limited depth of field, digital holographic microscopy (DHM) was used for the visualization. The field of view for all holograms was 9 mm × 9 mm. USAF resolution target was used to determine spatial resolution of the DHM. With the higher levels of magnification the three bar pattern could be seen as small as 5 μm. This method produces much better images because of the removal of all of the extra lenses. The dense spray region of the aerated liquid jet was divided into several investigation windows with a field of view of 9 mm × 9 mm, and double-pulsed holograms were recorded for each window with a 2048 × 2048 CCD double exposure sensor. Holograms digitally recorded on the CCD sensor have complete three-dimensional information. With the digital reconstruction process, three-dimensional information can be easily expressed with many two-dimensional slices. Thus, the entire flow field for any spanwise distance could be investigated by numerical reconstruction of original holograms. Original hologram and reconstruction hologram focused at the injector center plane is shown in Fig. 8. The original hologram was digitally recorded at the following test conditions: injector exit diameter (d_0) of 1 mm, gas to liquid ratio (GLR) of 8%, and jet/freestream momentum flux ratio (q_0) of 0.74. The original hologram and reconstruction hologram have the same

field of view of 9 mm × 9 mm. The entire spray structure of the dense spray region ($x/d_0 < 13.5$) could be visualized with six high resolution holograms reconstructed at the same spanwise depth as shown in Fig. 9. The aerated jet was injected into subsonic crossflow and bended in the crossflow direction. Most droplets detached from the liquid column of the aerated jet were non–spherical. Non-spherical droplets' distribution near the injector is shown in Fig. 8b. This explains why diagnostics like PDPA were not successful in probing the dense spray region of the aerated liquid jets.

B. Jet Surface Velocity

Liquid surface velocities in the injector exit would be small due to the effect of no-slip condition between the liquid and the wall inside injector. Further away from the nozzle exit surface velocity increases rapidly in the streamwise direction and then approaches constant value. Streamwise mean liquid surface velocities, v_s, were measured at the following test conditions: nozzle orifice diameter (d_0) of 1 mm, gas to liquid ratio (GLR) of 8%, and jet/freestream momentum flux ratio (q_0) of 0.74. The liquid surface velocities were measured with several double-pulsed holograms. The liquid surface velocities of aerated liquid jets as the function of streamwise distance are shown in Fig. 10. The surface velocities increase within the streamwise location of y/d_0=1.5~5.5 and then becomes nearly constant as the jet approaches the location of y/d_0=5.5. Liquid surface velocity obtained at y/d_0=6 approached the mean jet velocity.

C. Drop Sizes

The region of x/d_0= 0~18 and x/d_0= 0~22.5 was split into nine investigation windows to obtain spatial resolution of 5 μm and a reasonable field of view (9 mm × 9 mm). The spatial resolution of the current setup was 5 μm which allowed the size measurement of most droplets in the dense spray region. Droplets' sizes together with three-dimensional velocities were plotted as function of x-y-z location as shown in Fig. 11. Non-spherical droplets' diameter in the near-injector region was expressed by equivalent spherical diameter. The equivalent diameters were calculated as follows:

$$d_{eq} = (d_{max} \times d_{min})^{1/2} \tag{3}$$

where d_{max} and d_{min} are the major axis and the minor axis for an elliptical droplet, respectively. The sphericity for all droplets in the near-injector region could be expressed by dividing the major axis by the minor axis as shown in Fig. 12. The droplets in the near-injector region were mainly non-spherical which makes them inaccessible for techniques like PDPA. The sphericity is large near the injector exit, but decreases in the downstream region due to the surface tension effects. Moreover, most droplets at the downstream region have relatively small diameter possibly due to the secondary breakup effect. Sauter mean diameter (SMD) was measured at x/d_0 = 0, 9 and 18 for test conditions of: 8% GLR, q_0=0.74, d_0 = 1 mm, U_∞ = 61m/s. The SMD reduced with the increase in downstream distance as shown in Fig. 13. The reduction of the SMD in downstream region results from the secondary breakup. However, the SMD increased further away from the injector center plane due to the annular spray structure of the aerated liquid jet.

Droplet sizes normalized by their mass median diameter (MMD) satisfy Simmons' universal root normal distribution with MMD/SMD = 1.2 when plotted on a root-normal graph as shown in Fig. 14. The present study's data and previous data of Miller et al.[1] are shown in Fig. 14. The majority of these points fall on the line where the MMD/SMD = 1.2 (Simmons[13]). This agreement helps to validate the present experimental method. Finally the drop size distribution of aerated liquid jet in crossflow can be fully described by the SMD alone.

D. Droplets Velocities

The droplets velocities in the streamwise and the crossflow direction could be measured by observing the displacements of the center of each droplet between the double pulses. The spanwise velocity could be measured by observing the change of the planes of focus measured between the double pulses. The time interval between the two laser pulses was controlled by a delay generator. An oscilloscope and a photo detector were used to measure the time interval between the double pulses. Typical double-pulsed hologram used for three dimensional velocities' measurement is shown in Fig. 15. The time interval between these two laser pulses was 47 μs. The double-pulsed hologram was obtained at the following location: x/d_0=4.5~13.5 and y/d_0=18~27. Three individual droplets marked with three capital letters ("A," "B," and "C") on two holograms reconstructed at the different spanwise distances

have different displacements in the streamwise and cross stream directions. The droplets marked with the letter C and the letter C' were respectively focused at two different spanwise depths of z/d_0= -1 and z/d_0= -1.167. Droplets spanwise velocities were obtained by measuring the spanwise distance between the two focused planes and the time interval between the double pulses. The droplet marked with "C" has negative spanwise velocity, because the droplet has receded from the injector center plane during the double pulses. It is plausible because the liquid sheet of the aerated jet with hollow-type structure spreads toward both positive and negative direction away from the injector center plane. This three-dimensional velocity measurement was performed for all individual droplets in nine investigation windows in the near-injector region.

Mass averaged velocities in the streamwise and cross stream directions, $\tilde{u}$ and $\tilde{v}$, have been measured within the spanwise distance of z/d_0= -13~13. The mass averaged cross stream velocities normalized by the free crossflow velocity, $\tilde{u}/u_\infty$, are shown in Fig. 16. The mass averaged cross stream velocities increase with downstream distance due to the interaction between the crossflow and the droplets, and approach the crossflow velocity, u_∞, further away from the injector. The mass averaged streamwise velocities normalized by the mean aerated liquid jet velocity, $\tilde{v}/v_{jet}$ are shown in Fig. 17. The mass averaged streamwise velocities decreases further away from the injector exit.

The cross stream droplets velocity distribution as function of droplets' sizes is shown in Fig. 18. The cross stream droplets velocity, u, was normalized by the mass averaged cross stream velocity, $\tilde{u}$, and droplets sizes are normalized by the SMD. The cross stream velocities of smaller droplets are higher than the mass averaged cross stream velocity, and the cross stream velocities of bigger droplets are lower than the mass averaged velocity. This can be attributed to the effect of the mass of each droplet. The relationship between the cross stream velocities normalized by the mass averaged cross stream velocity and the droplet sizes normalized by the SMD is expressed as follows:

$$u/\tilde{u} > 1, \text{ for } d/SMD > 0.8 \tag{5}$$

$$u/\tilde{u} = 1, \text{ for } 0.8 < d/SMD < 1.2 \tag{6}$$

$$u/\tilde{u} < 1, \text{ for } d/SMD > 1.2 \tag{7}$$

The streamwise droplets velocity distribution normalized by the mass averaged streamwise velocity, $\tilde{v}$, as the function of droplets sizes normalized by the SMD is shown in Fig. 19. The streamwise droplets velocities, $v/\tilde{v}$ is unity for droplet sizes normalized by the SMD greater than 0.4.

The spanwise droplets velocities normalized by the mass averaged spanwise velocity, $\tilde{w}$, as function of droplets sizes normalized by the SMD are shown in Fig. 20. The spanwise droplets velocities were not influenced by d/SMD, unlike the stramwise and crossflow velocities.

IV. Conclusions

The near-injector region (x/d_0= 0~22.5, y/d_0= 0~27) of aerated liquid jet in subsonic crossflow was investigated by double-pulsed digital holographic microscopy (DHM) for the following test conditions: jet exit diameter of 1 mm, GLR = 8% and momentum flux ratio of 0.74. The holograms were recorded on CCD sensor with a spatial resolution of 5 μm, and were numerically reconstructed at different span wise distances. To overcome the limited field of view of DHM, the near-injector region has been divided into several investigation windows. To visualize the entire structure of aerated liquid jet, a spray map was constructed by patching several reconstruction holograms with high resolution. Individual droplets' sizes, locations, and three-dimensional velocities were measured. Mass averaged velocities' distributions were obtained as function of droplets sizes normalized by the Sauter mean diameter (SMD). The major conclusions of the present study are as follows:

1) Digital holographic microscopy is suitable for probing the dense spray near-injector region for aerated liquid jets in subsonic crossflow. The present optical setup is relatively simple and does not require a collimating lens or relay lens unlike digital in-line holography, which helps increase the resolution of the technique.

2) Large field of view can be obtained by simply patching several high resolution holograms reconstructed at the same span wise distance.

3) Droplets velocities in three-dimensions are measured by tracking their displacements during the time interval between the double-pulses in the stream wise and cross stream direction and by tracking the change in the plane of focus in the span wise direction.

4) Most droplets in the probed region are non-spherical. The droplets were considered elliptical in shape and were characterized by their equivalent "spherical diameter".

5) The distributions of the stream wise and cross stream velocities were uniform in the near-injector region and could be characterized by the mass-average velocity except for very small and very large droplets.

6) The drop size distributions of aerated liquid jet in crossflow for the present test conditions (i.e., GLR 8%) followed Simmons' universal root normal distribution (Simmons[13]) and thus could be fully described by the SMD alone.

Acknowledgments

Support from Taitech, Inc., under a subcontract with the U.S. Air Force Research Laboratory is gratefully acknowledged. Initial development of experimental methods was carried out under the National Science Foundation grant EPS-0132534 (Oklahoma-EPSCOR). The U.S. government is authorized to make copies of this article for governmental purposes notwithstanding any copyright notation thereon.

References

[1]Miller, B., Sallam, K. A., Bingabr, M., Lin, K.-C. and Carter, C. D. "Breakup of Aerated Liquid Jets in Subsonic Crossflow," J. Prop. Power, in press.

[2]Kim, J. Y., and Lee, S. Y., "Dependence of Spraying Performance on the Internal Flow Pattern in Effervescent Atomizers," *Atomization and Sprays*, Vol. 11, 2001, pp. 735–756.

[3]Lefebvre, A. H., Wang, X.F., and Martin, C. A., "Spray Characteristics of Aerated-Liquid Pressure Atomizers," *Journal of Propulsion*, Vol. 4, 1988, pp. 293-298.

[4]Buckner, H. N., and Sojka, P.E., "Effervescent Atomization of High-Viscosity Fluids: Part I. Newtonian Liquids," *Atomization and Sprays*, Vol. 1, 1991, pp. 239-252.

[5]Lund, M. T., Sojka, P. E., Lefebvre, A. H., and Gosselin, P.G., "Effervescent Atomization at Low Mass Flow Rates Part 1: The Influence of Surface Tension," *Atomization and Sprays*, Vol. 3, 1993, pp. 77-89.

[6]Santangelo, P. J., and Sojka, P. E., "A Holographic Investigation of an Effervescent Atomizer-Produced Spray," *Atomization and Sprays*, Vol. 5, 1995, pp. 137-155.

[7]Sutherland, J. J., Sojka, P. E., and Plesniak, M. W., "Entrainment by Ligament Controlled Effervescent Atomizer Produced Sprays," *Int. J. Multiphase Flow*, Vol. 23, 1996, pp. 865-884.

[8]Wade, R. A., Weerts, J. M., Sojka, P. E., Gore, J. P., and Eckerle, W. A., "Effervescent Atomization at Injection Pressures in the MPa Range," *Atomization and Sprays*, Vol. 9, No. 6, 1999, pp. 651-657.

[9]Lin, K.-C., Kennedy, P. J., and Jackson, T. A., "Spray Structures of Aerated-Liquid Jets in Subsonic Crossflows," *32nd AIAA Aerospace Sciences Meeting*, AIAA Paper 2001-0330, 2001.

[10]Lin, K.-C., Kennedy, P. J., and Jackson, T. A., "Structures of Aerated Liquid Jets in High Speed Crossflows," *32nd AIAA Fluid Dynamics Conference*, AIAA Paper 2002-3178, 2002.

[11]Sallam, K. A., Aalburg, C., Faeth, G. M., Lin, K.-C., Carter, C. D., and Jackson, T. A., "Primary Breakup of Round Aerated-Liquid Jets in Supersonic Crossflows," *Atomization and Sprays*, Vol. 16, No. 6, 2006, pp. 657–672.

[12]Schnars, U., and Jueptner, W., *Digital Holography: Digital Hologram Recording, Numerical Reconstruction, and Related Techniques*, Springer, Berlin, 2005.

[13]Simmons, H. C., "The Correlation of Drop-Size Distributions in Fuel Nozzle Sprays," *Journal of Engineering for Power*, Vol. 99, No. 3, 1977, pp. 309–319.

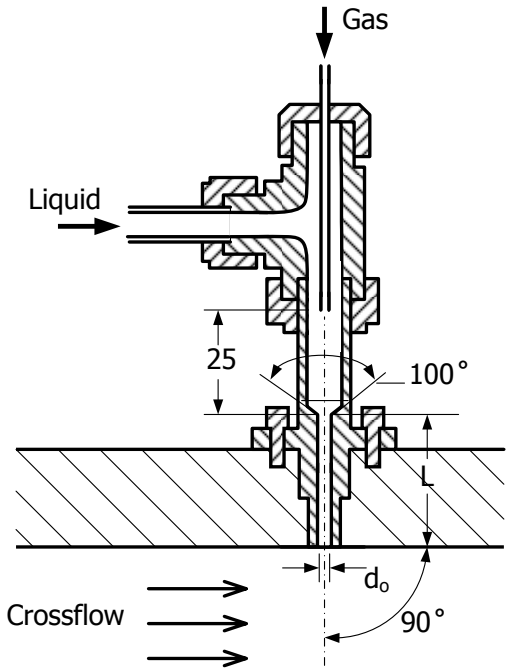

Figure 1. Schematic of an aerated injector (inside out setup shown from (ref. 9)).

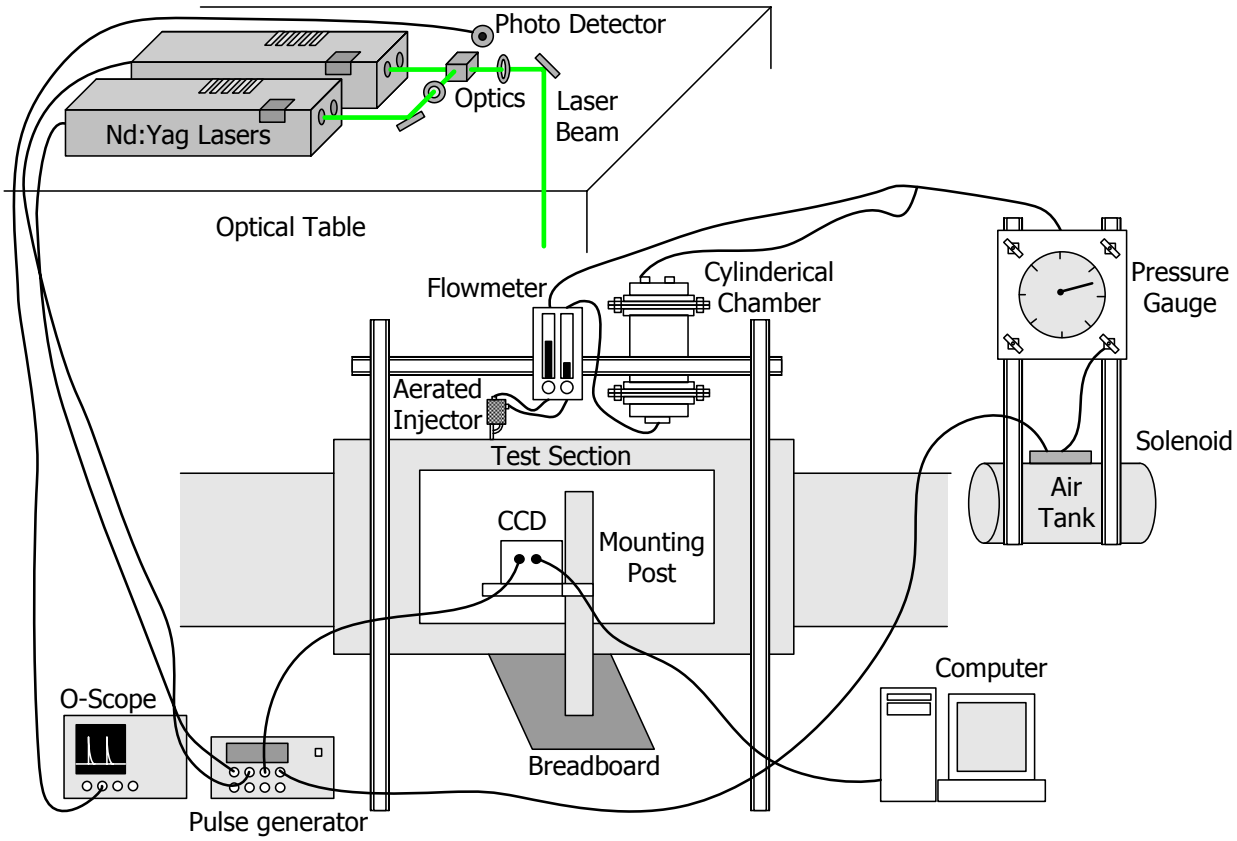

Figure 2. Experimental apparatus.

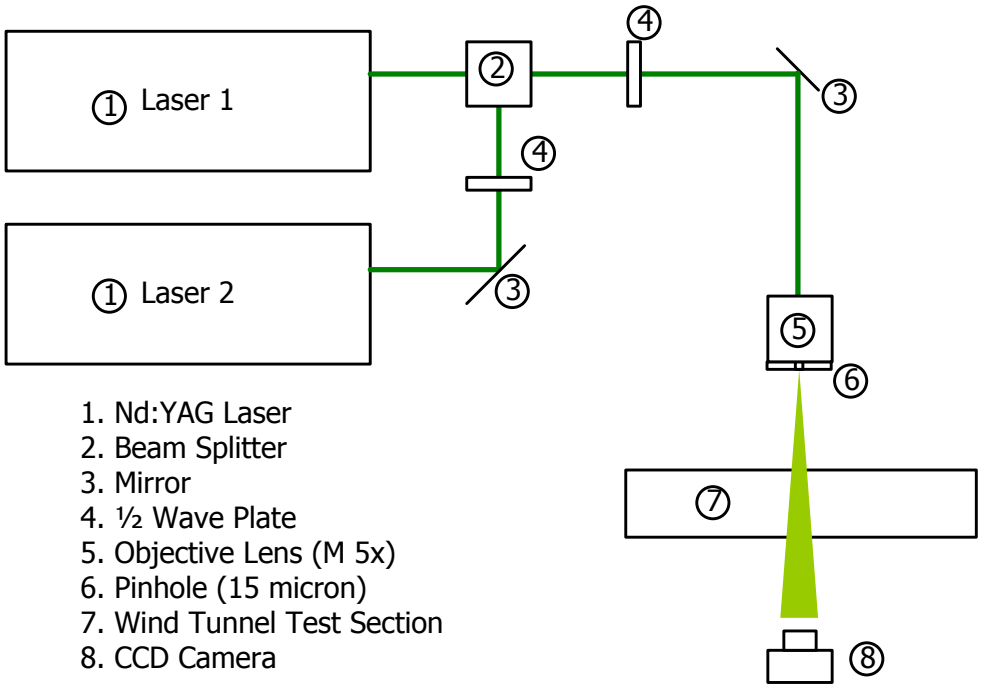

Figure 3. Optical setup for digital holographic microscopy (DHM).

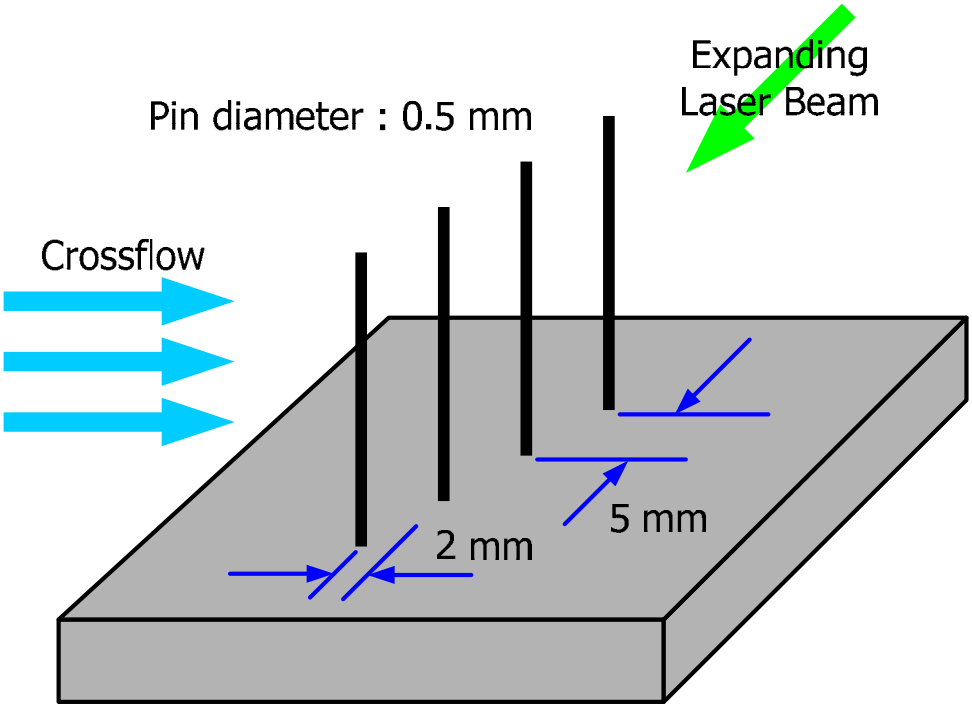

Figure 4. Schematic of four pins for spatial calibration.

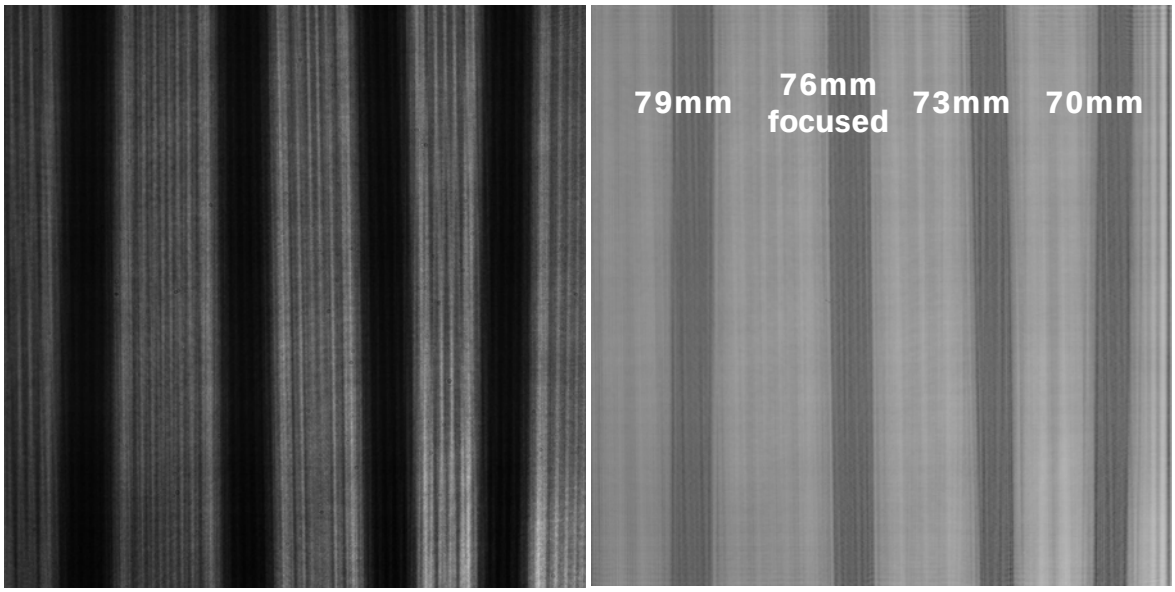

a) b)

Figure 5. Hologram a) recorded for spatial calibration and b) reconstructed at the spanwise depth of 76 mm from CCD sensor.

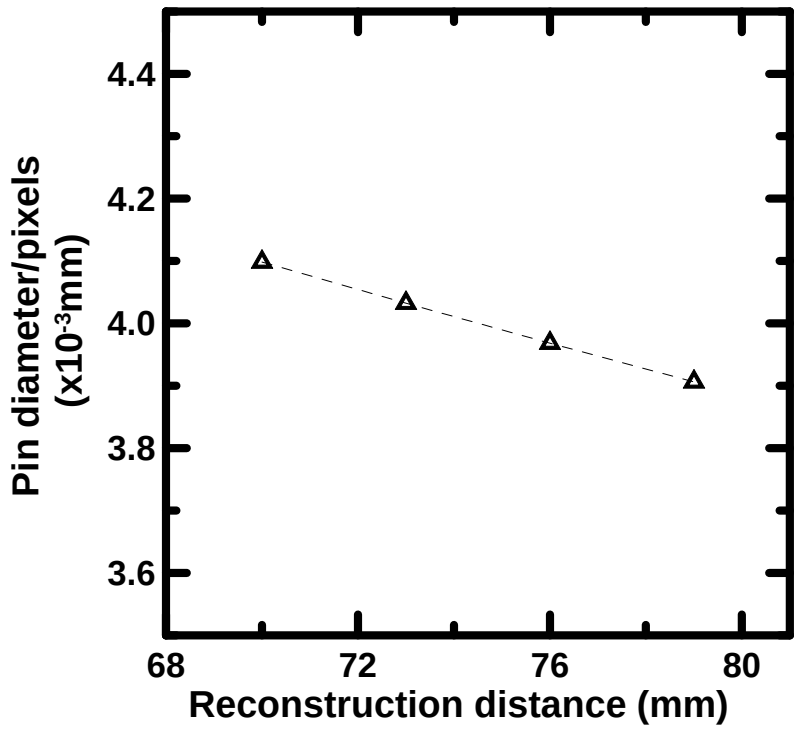

Figure 6. Spatial calibration between actual distance and pixel numbers for all reconstruction distances within the field of view.

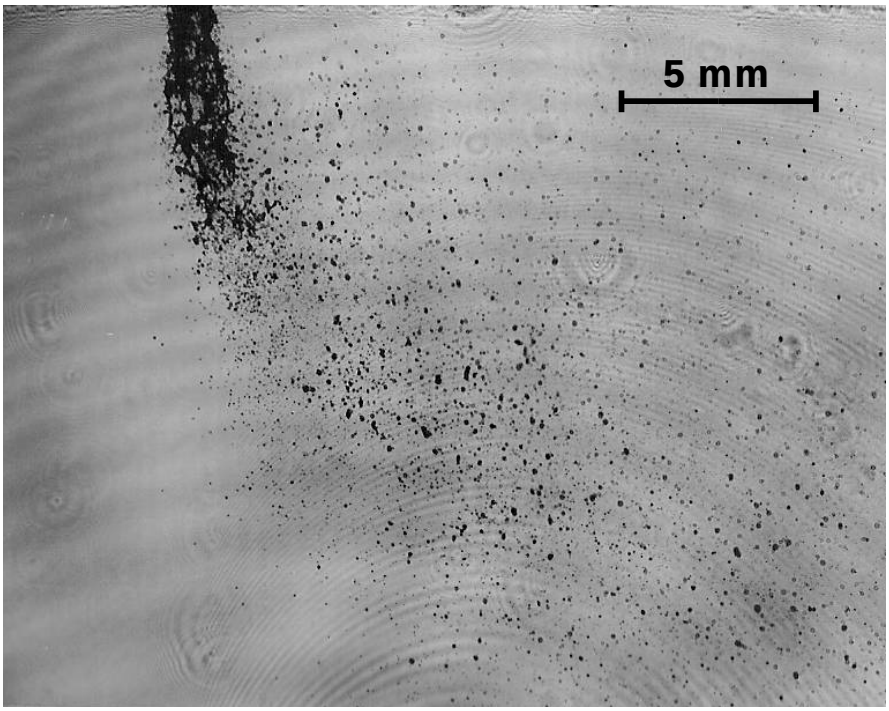

Figure 7. Pulsed shadowgrpahy of aerated liquid jet in subsonic crossflow (Test condition: 1mm jet diameter, 8% GLR, and q_0=0.74).

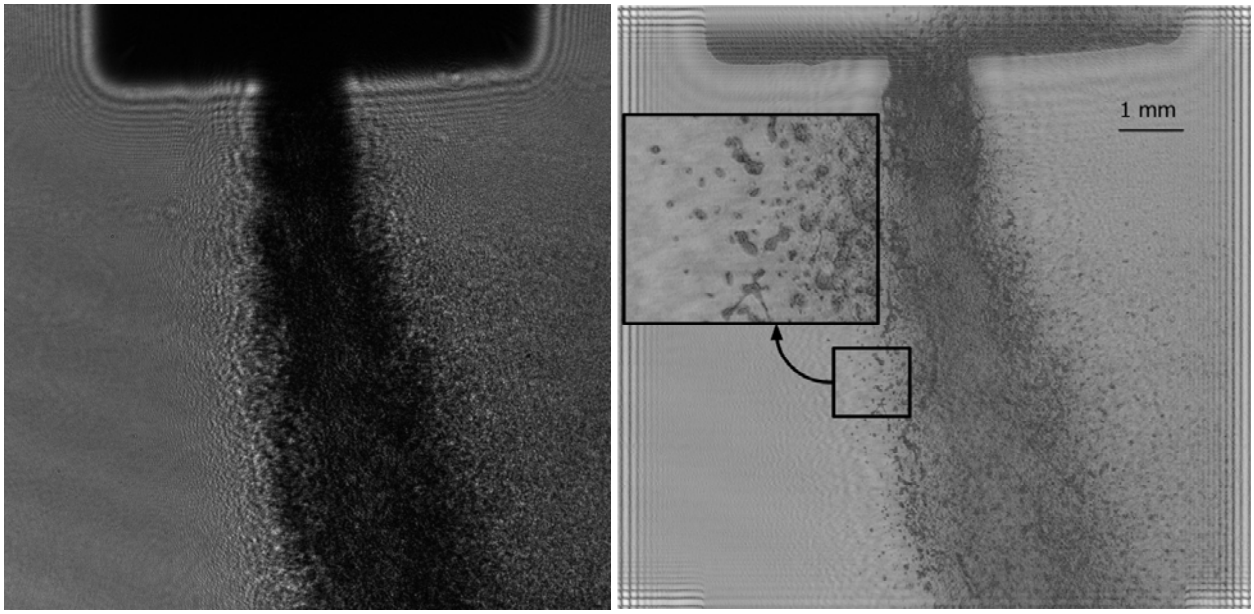

Figure 8. Hologram a) recorded at the location of x/d_0 = -4.5 ~ 4.5 and y/d_0 = 0 ~ 9 (gaseous crossflow comes from left to right, Test condition: GLR = 8%, jet exit diameter d_0 = 1mm, and q_0 = 0.74) and b) reconstructed at the spanwise depth of 72 mm from CCD sensor: the inset shows an enlarged image of the small rectangular region.

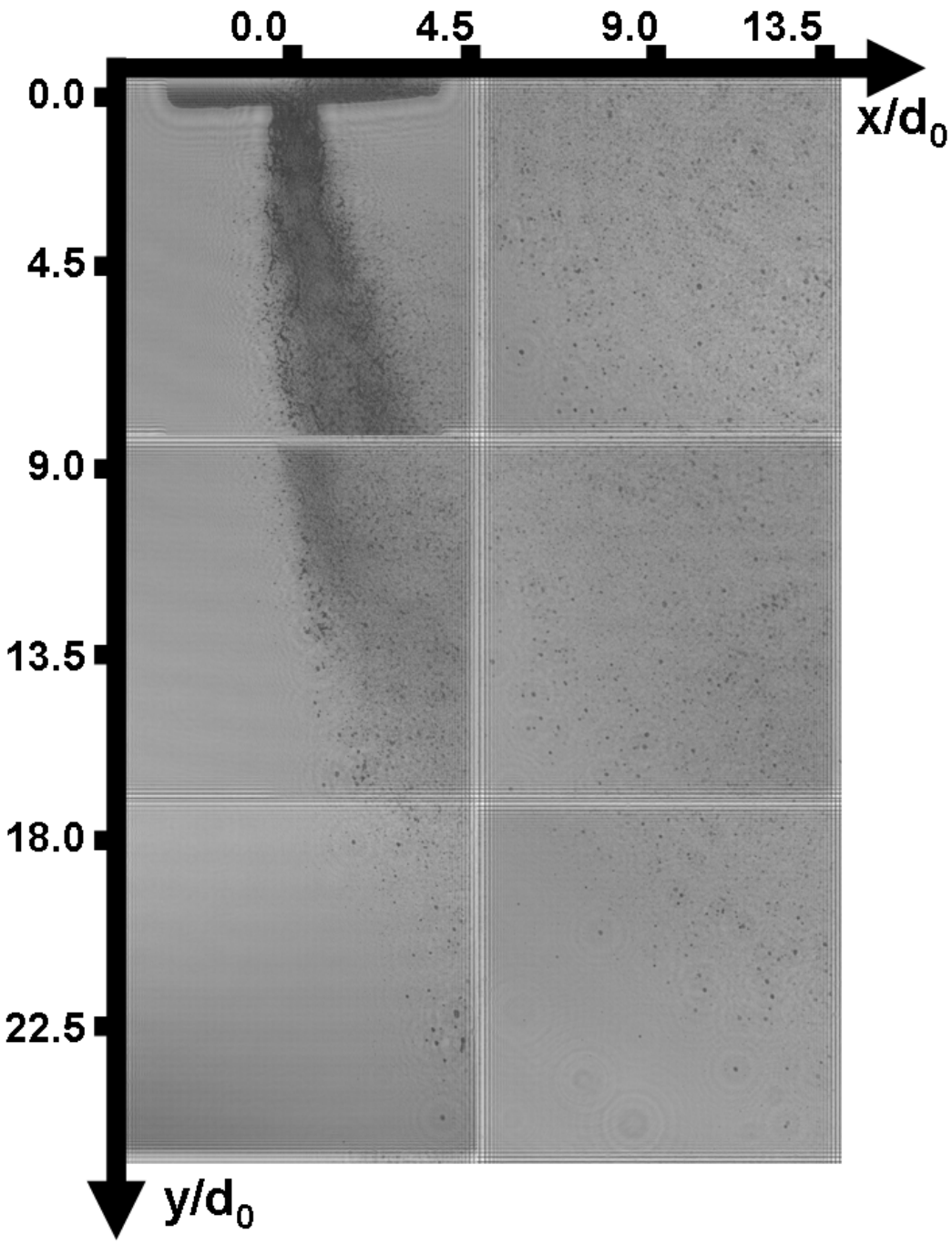

Figure 9. Aerated liquid jet spray structure near injector region.

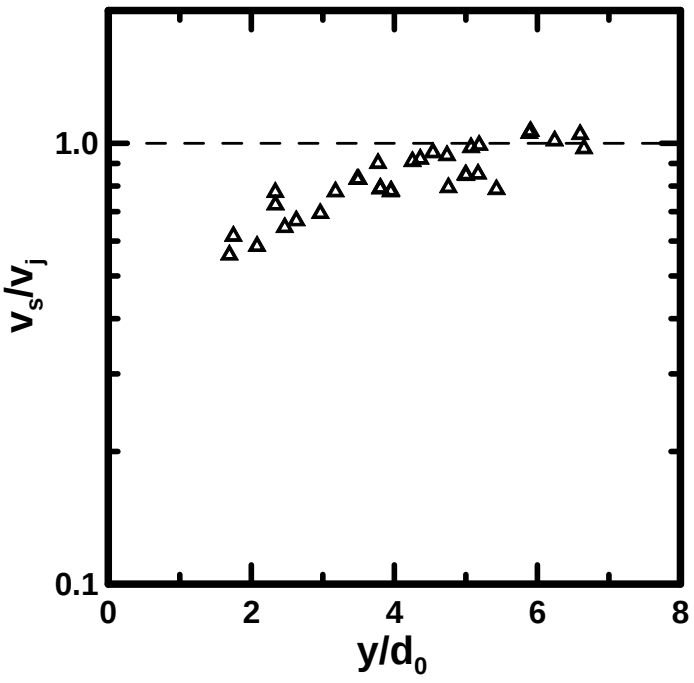

Figure 10. Variation of surface velocity of liquid sheet column ejected from the injector exit for streamwise distance.

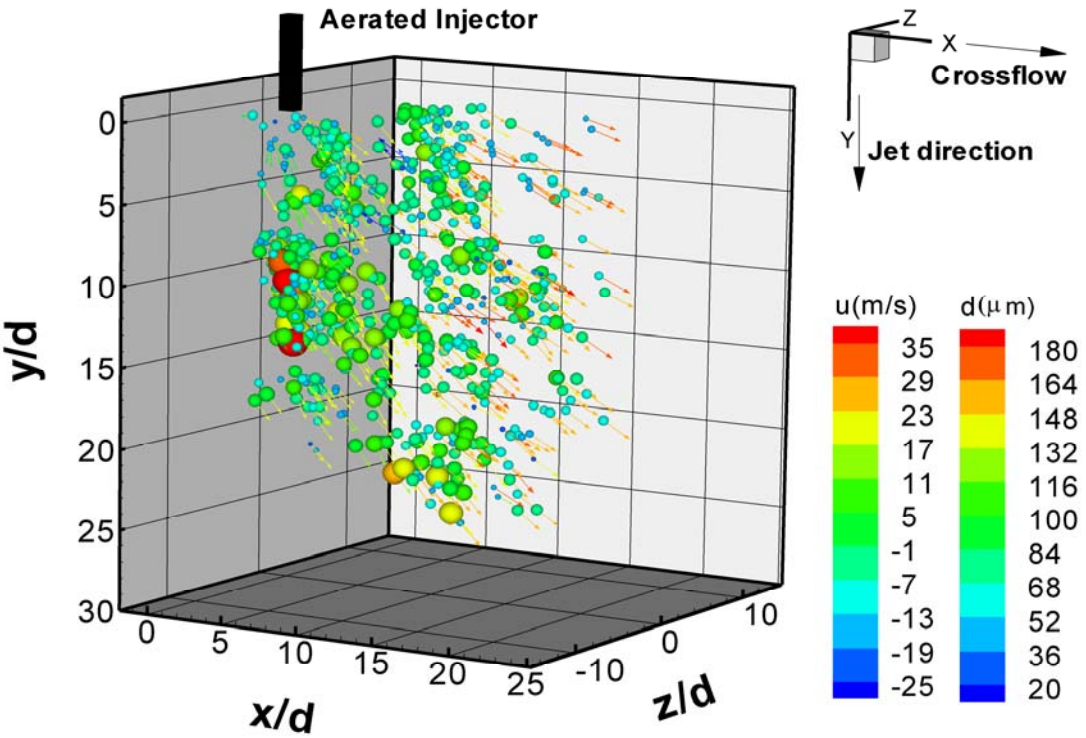

Figure 11. Drop size distribution and three-dimensional velocities near injector region.

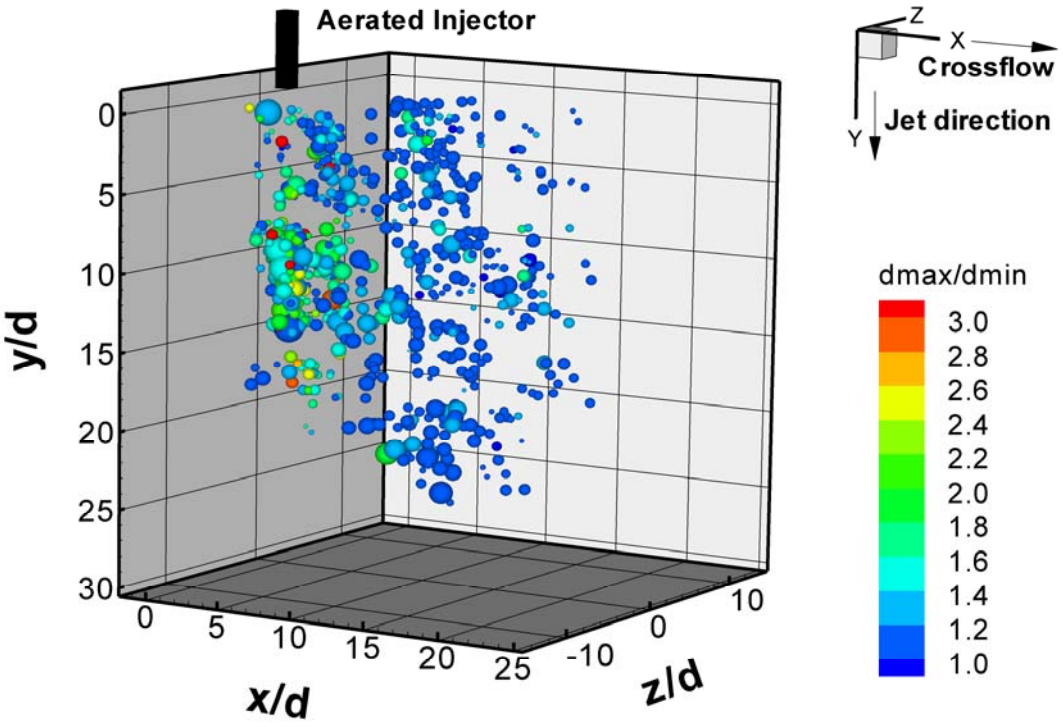

Figure 12. Sphericity of individual Droplets near very injector.

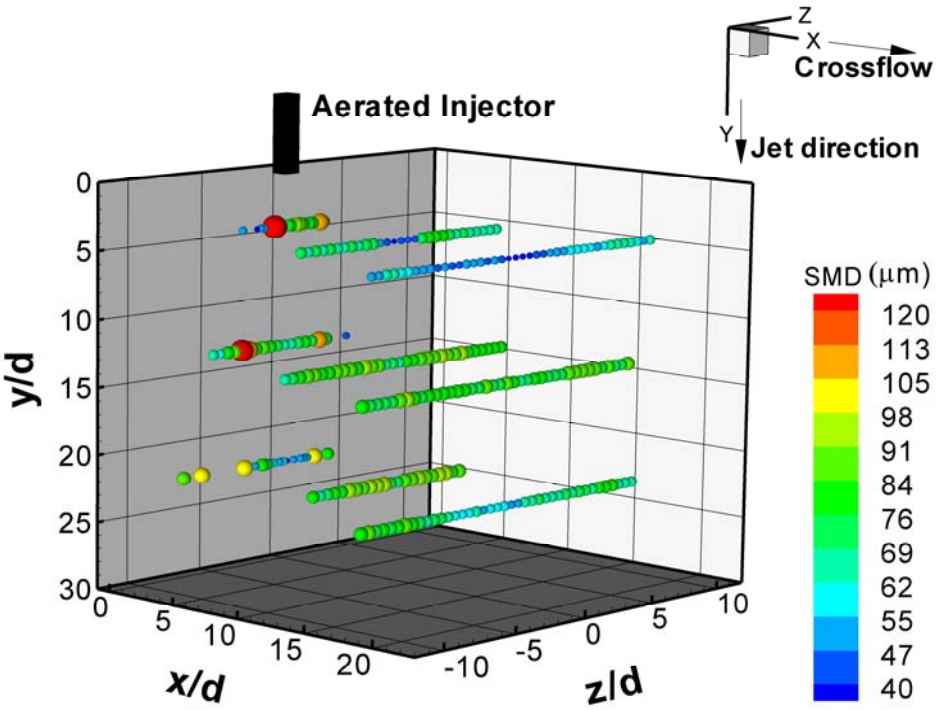

Figure 13. Sauter mean diameter (SMD) distribution near injector.

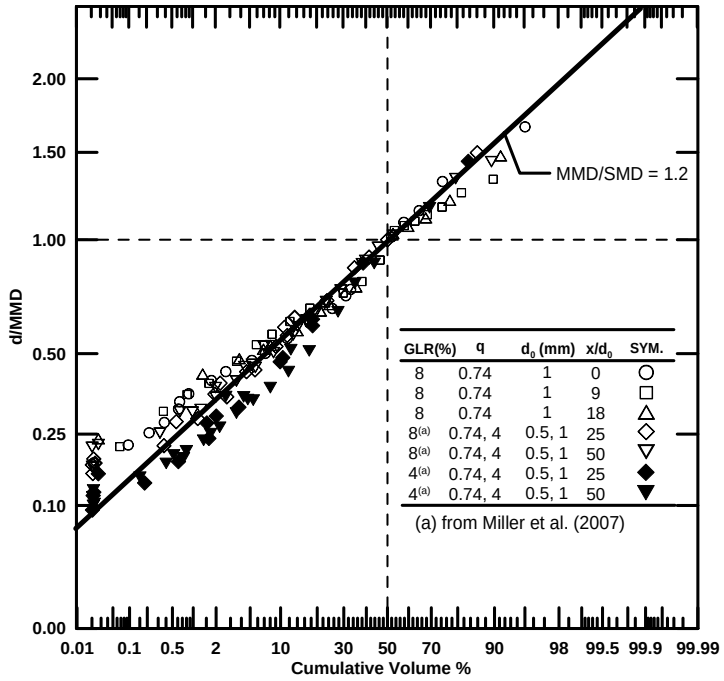

Figure 14. Droplet size distribution.

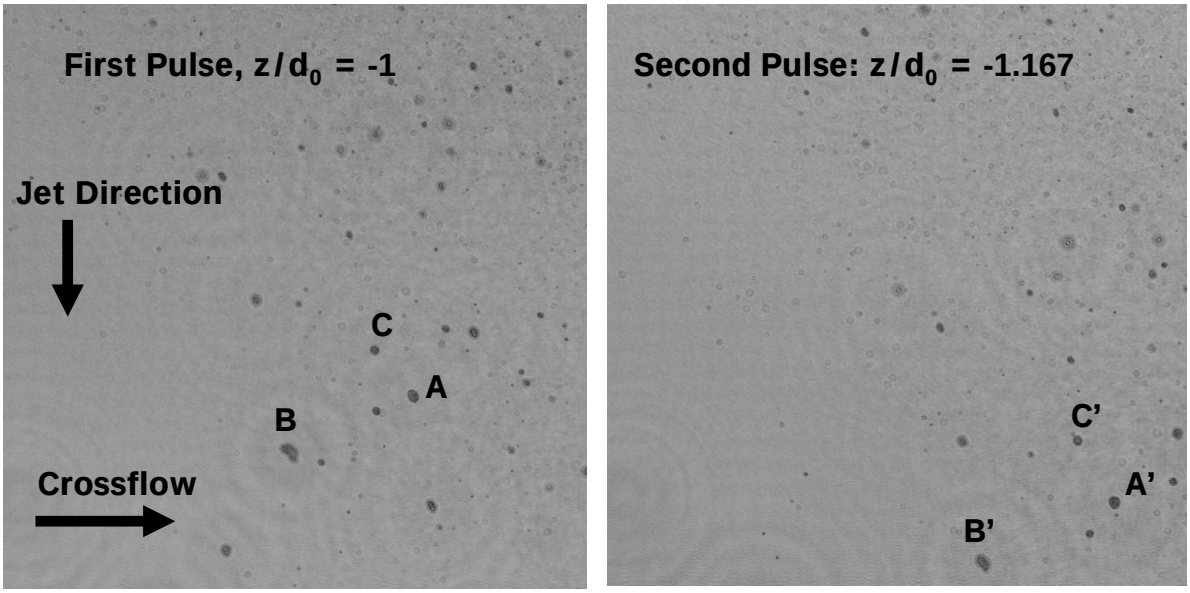

Figure 15. Double-pulsed reconstructed hologram at (a) t = 0 and (b) t = 47 μs. Test condition are : GLR = 8%, q_0 = 0.74 at x/d_0 = 9 and y/d_0 = 22. The letters "A," "B," and "C" refer to distinct droplets that are tacked between the two pulses to yield velocity information.

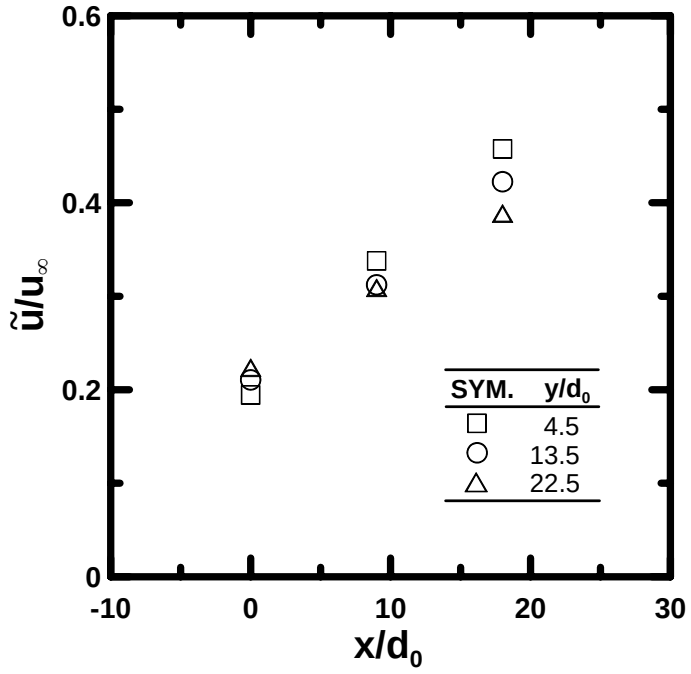

Figure 16. Mass averaged cross stream droplets velocities for different x/d_0 locations.

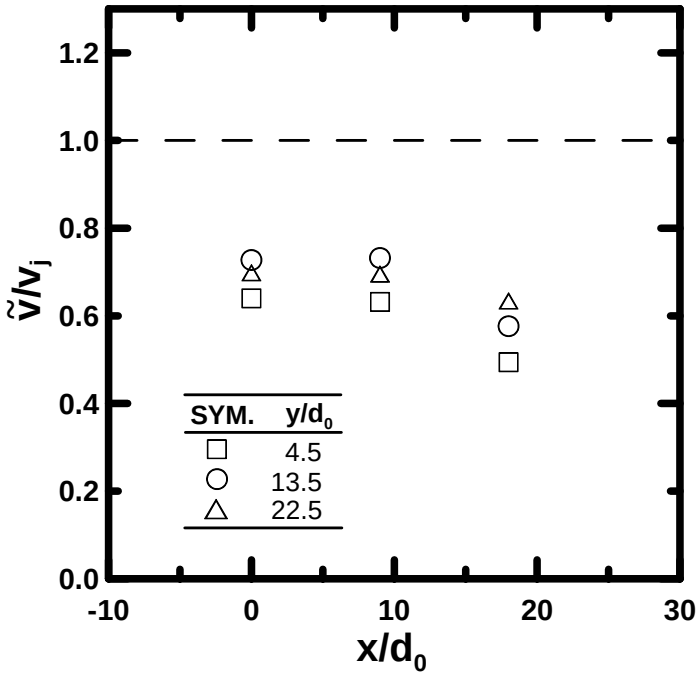

Figure 17. Mass averaged streamwise droplets velocities for different x/d_0 locations.

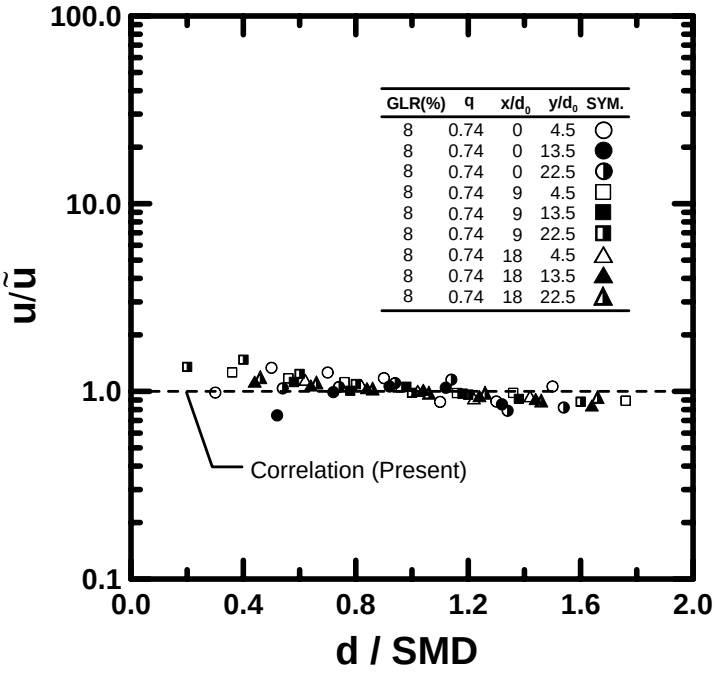

Figure 18. Cross stream droplets' velocity distribution normalized by mass averaged cross stream velocity as function of droplets' sizes.

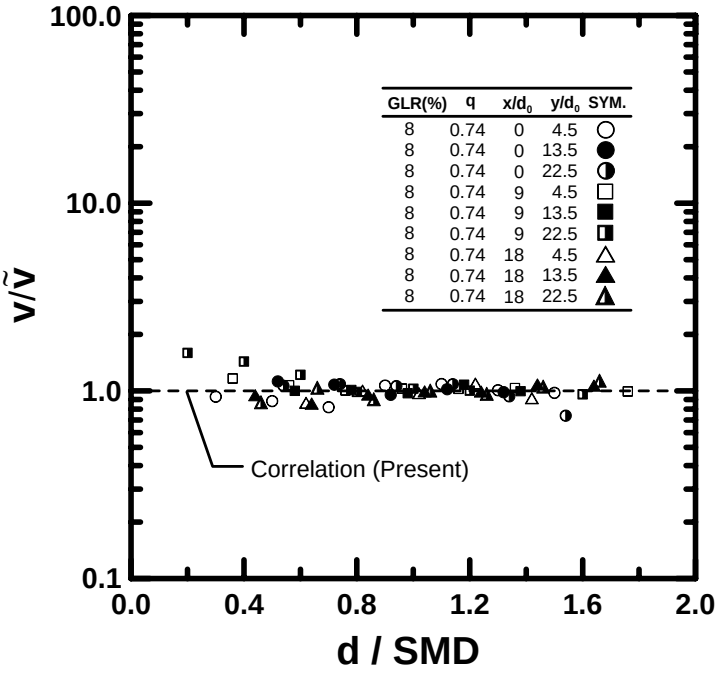

Figure 19. Streamwise droplets' velocity distribution normalized by mass averaged streamwise velocity as function of droplets' sizes.

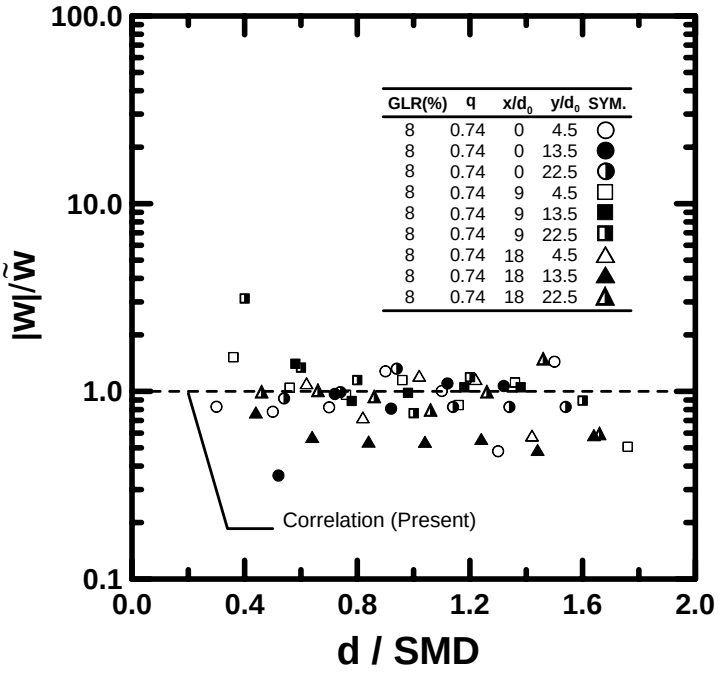

Figure 20. Spanwise droplets' velocity distribution normalized by mass averaged spanwise velocity as function of droplets' sizes.